Torus Construction and Quantization for the Hydrogen Atom in Crossed Electric and Magnetic Fields

Stephan Gekle and Jörg Main
Institut für Theoretische Physik 1, Universität Stuttgart, 70550 Stuttgart, GERMANY

Thomas Bartsch
Center for Nonlinear Science, Georgia Institute of Technology, Atlanta, Georgia 30332-0430, USA
(Received 17 March 2006)

Periodic orbits of the hydrogen atom in crossed electric and magnetic fields are shown to obey an organizing principle. This principle allows us to assign winding numbers to the periodic orbits and to quantitatively construct the action variables for broken tori in phase space. We carry out an EBK torus quantization at energies below and above the ionization saddle point.

PACS numbers: 05.45.-a, 05.45.Jn, 45.20.Jj, 32.60.+i
Keywords: periodic orbits, torus construction, EBK torus quantization, phase space topology

1. Introduction

The pivotal role of periodic orbits for the study of dynamical systems was diagnosed by Henri Poincaré as early as 1892 [1]: "In fact, what makes these periodic solutions so precious to us, is that they are, so to speak, the only breach through which we can try to penetrate in a place which, up to now, was thought to be inaccessible." [a]

Indeed, today periodic motion is widely recognized as the most prominent feature in a wide range of dynamical systems, from astronomy [1–3], molecular vibrations [4, 5], chemical reactions [6], particle accelerators [7], atomic and molecular physics [8–10] to fluid dynamics, e.g., statistics of turbulent flow [11]. While most research to date has focused on either two-degree-of-freedom systems or selected periodic orbits in high-dimensional systems, our purpose here is to understand the governing principles behind the organization of periodic orbits in their entirety. The completion of this challenging and laborious task is the key to the intricate geometrical and dynamical structure of the multidimensional phase space.

In this work we establish an organizing principle for periodic orbits in a multidimensional non-integrable Hamiltonian system that allows the identification of winding numbers for every periodic orbit (PO) originating from the breakup of an invariant torus. These periodic orbits determine the structures of the phase space and allow one to characterize their topology as well as their symmetries. These structures are the remnants of invariant tori and thus serve as the basis for an Einstein-Brillouin-Keller (EBK) torus quantization [12–14]. We illustrate our method for the hydrogen atom in crossed electric and magnetic fields at energies below and above the ionization threshold. This system serves as a paradigm of strongly coupled multidimensional systems because it can be investigated both experimentally and theoretically [9, 10, 15]. However, after two decades of intense scrutiny, the overall phase space structure still defies a complete understanding. In particular, no pertinent symbolic dynamics are known. Due to the intimate connection between the crossed-fields hydrogen atom and the restricted three-body problem of celestial mechanics [16, 17], we expect that

[a] "D'ailleurs, ce qui nous rend ces solutions périodiques si précieuses, c'est qu'elles sont, pour ainsi dire, la seule brèche par où nous puissions essayer de pénétrer dans une place jusqu'ici réputée inabordable."

the method of this paper will elucidate the ordering principle of POs in that famous problem. A deeper understanding of the hydrogen atom in external fields also provides a solid basis to explore the behavior of confined electrons in condensed matter physics, such as in excitons [18] and quantum dots [19].

2. Phase space topology

In integrable systems any motion is confined to an invariant torus [20] characterized by a set of actions $\mathbf{I}$ that are the constants of motion. Their conjugate angles $\boldsymbol{\theta}$ determine the position on the torus. Finding the action-angle coordinates explicitly, however, is a highly non-trivial task. Due to its relevance to quantization, this problem has attracted considerable attention [21, 22]. If the torus is resonant, i.e., any two of the frequencies $\boldsymbol{\omega} = d\boldsymbol{\theta}/dt$ have a rational ratio, it carries periodic orbits for which integer winding numbers $\mathbf{w}$ can be defined such that $\omega_i/\omega_j = w_i/w_j$.

In a non-integrable system, a resonant torus breaks up into isolated POs [20, 23]. We use these POs as representatives of the torus they stem from and call them N-torus POs, where N is the dimension of the original torus. According to Kolmogorov-Arnold-Moser (KAM) theory [20], most nonresonant tori remain intact and break up only gradually. They are interspersed with the isolated POs in the same way as resonant and nonresonant tori are interspersed in an integrable system. Therefore, POs can be used to investigate the structure of the surviving tori. POs that do not originate from the breakup of an invariant torus will not be considered further.

We determine this topology quantitatively for the hydrogen atom in an electric field F in the x direction and a magnetic field B in the z direction. The Hamiltonian for the electronic motion reads, in atomic units,

$$H = \frac{1}{2}\mathbf{p}^2 - \frac{1}{r} + \frac{B}{2}\left(p_y x - p_x y\right) + \frac{B^2}{8}\left(x^2 + y^2\right) - Fx. \tag{1}$$

Here x, y, z, p_x, p_y, p_z are the usual Cartesian coordinates and momenta, and $r = \sqrt{x^2 + y^2 + z^2}$.

By virtue of the scaling properties [24] of the Hamiltonian (1), if all classical quantities are multiplied by suitable powers of the magnetic field strength, the dynamics can be shown not to depend on the energy E and the field strengths B and F separately, but only on the scaled energy $\tilde{E} = B^{-2/3}E$ and the scaled electric-field strength $\tilde{F} = B^{-4/3}F$. In particular, coordinates scale according to $\tilde{\mathbf{r}} = B^{2/3}\mathbf{r}$ and the classical actions obey $S = B^{-1/3}\tilde{S}$. We take the scaled electric field strength $\tilde{F} = 0.5$ and consider two scaled energies, $\tilde{E} = -1.5$ and $\tilde{E} = -1.4$, slightly below and slightly above the ionization threshold $\tilde{E}_{\mathrm{I}} = -2\sqrt{\tilde{F}}$. This choice guarantees strong coupling between the three degrees of freedom. The scaled coordinates and momenta also carry a tilde.

The Hamiltonian (1) has three discrete symmetries, namely the reflection symmetry with respect to the xy plane (z-parity), the y-parity with additional time reversal and the combination of both. Due to the z-parity, the xy plane constitutes a two-degree-of-freedom subsystem. Any PO outside this plane must either be invariant under the symmetry transformation or possess a partner related to it via the symmetry transformation.

The hierarchy of N-torus POs at the two energies is almost identical. Three fundamental periodic orbits (FPOs), shaped almost like Keplerian ellipses, were found in [25]. They do not arise from the breakup of a higher-dimensional torus and therefore represent the 1-torus POs in the hierarchy. Two of these, labeled S^+ and S^- in [16], serve as organizing centers for two families of 2-torus POs, which we call T_2^{p} and T_2^{n}. The POs located in the xy symmetry plane form the T_2^{p} family. The 2-torus POs themselves are found to be limiting cases of two families T_3^{p} and T_3^{n} of 3-torus POs.

Figure 1 shows the scaled actions $\tilde{S}$ and scaled periods $\tilde{T}$ of POs that arise from the breakup of invariant tori. POs that are remnants of the same torus have nearly identical periods and actions, thus each point in Fig. 1 represents

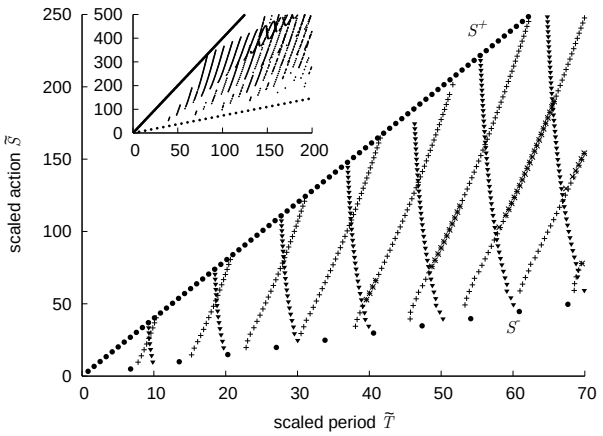

FIG. 1. Periodic orbits at $\tilde{E} = -1.4$ FPOs and their repetitions are shown with circles, T_2^{p} POs with plus symbols, T_2^{n} with triangles, T_3^{p} with crosses, and T_3^{n} with diamonds. The inset presents the 3-torus POs in an enlarged $\tilde{T}$-$\tilde{S}$ range.

the POs generated from a single torus. The FPOs $S^{\pm}$ and their repetitions lie on boundary lines that enclose the non-fundamental POs. The latter are arranged in series with positive or negative slopes in the $\tilde{T}$-$\tilde{S}$-diagram. These series form the $T_{2,3}^{\mathrm{p}}$ and $T_{2,3}^{\mathrm{n}}$ families, respectively. The existence of these series makes it easy to identify POs that are not part of the original torus structure and thus must be disregarded in the following.

Winding numbers for the 2-torus POs T_2^{p} and T_2^{n} can be assigned as follows: counting the series in Fig. 1 yields the first winding number w_1. Since the repetitions of the POs in the leftmost series can be found in all higher series, this first series must be assigned $w_1 = 1$. Counting the POs within one series from bottom to top yields the second winding number w_2. The base value w_2^0 to be assigned to the PO with the lowest action in the first series, however, remains undetermined from Fig. 1.

To determine w_2^0 we use Fourier expansions for the time series of periodic orbits in Cartesian coordinates. They provide us with various possible coordinate systems for the angle variables related to different sets of winding numbers. The system we call $\mathbf{w}$ is characterized by $w_2^0 = 2$, the system $\mathbf{w}'$ by $w_2^0 = 4$. These choices correspond to the two systems of angle coordinates imposed by the FPOs S^+ and S^-, respectively. Details of this procedure are given elsewhere [26].

Apart from the 2-torus POs T_2, Fig. 1 shows POs that come from the destruction of 3-tori. They fall into the same series as the 2-torus POs, and each 3-torus PO in the families T_3 is intimately related to a partner from T_2. Such partners have identical winding numbers w_1 and w_2, but 3-torus POs possess a third winding number w_3. The latter manifests itself in an additional peak in the Fourier spectra and therefore can be assigned by a straightforward extension of the technique used to classify the 2-torus POs. Again, the assignment of winding numbers corresponds to the choice of a system of angle coordinates and is not unique.

We find the following connection between winding numbers and symmetry. In the T_3^{p} family exactly those POs with w_1 and w_2 even are symmetric under the z-parity transformation. In the T_2^{n} and T_3^{n} families exactly those POs with w_1 odd and w_2 even are symmetric, while all others are not. For both families of 3-torus POs the third winding number w_3 has no influence on the symmetry properties.

Using the winding numbers $\mathbf{w}$, the total action can be written as $S = \mathbf{w} \cdot \tilde{\mathbf{I}}(\mathbf{w})$, where $\tilde{\mathbf{I}}(\mathbf{w})$ are the action coordinates. In fact, the actions depend only on the ratios of winding numbers (which equal the frequency ratios), e.g., w_1/w_2 and w_3/w_2 for the 3-torus POs or w_1/w_2 for the 2-torus POs. For the latter we obtain the action coordinates $\tilde{\mathbf{I}}$ shown in Fig. 2 together with the actions and stability angles $\phi_{1,2}$ (these are the phase angles of the unimodular eigenvalues of the stability matrix) of the FPOs $S^{\pm}$. These angles describe the rotations that an FPO imposes onto its neighborhood. The limiting values for high frequency ratios of the T_2^{p} and T_2^{n} families coincide with $\phi_1/2\pi$ and $\phi_2/2\pi$ of S^-, respectively. This shows how the T_2^{p} and T_2^{n} collapse onto S^- in two different directions. As the maximum frequency ratio is approached, $\tilde{I}_2$ converges towards the action of the FPO, whereas $\tilde{I}_1$ vanishes. These findings demonstrate that the loop

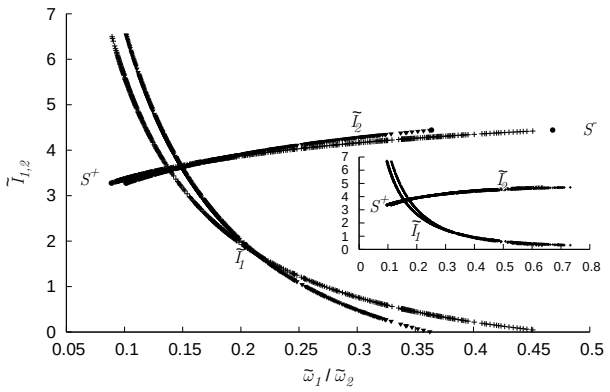

FIG. 2. Action variables for the T_2^{p} (plus symbols) and the T_2^{n} (triangles) families at $\tilde{E} = -1.5$ below the ionization threshold. Black dots show actions and stability angles of the FPOs S^+ and S^-. The inset presents an analogous graph at $\tilde{E} = -1.4$

in the θ_1 direction is transverse to the FPO S^- and shrinks to a point, whereas the loop in the θ_2 direction approaches the FPO itself.

The winding numbers $\mathbf{w}$ used in Fig. 2 are ill-suited to describe the approach to S^+, and indeed neither of the actions $\tilde{I}_1$ and $\tilde{I}_2$ tends to zero in the limit of low frequency ratios. Nevertheless, S^+ can be located in Fig. 2 with its stability angles transformed to the $\mathbf{w}$ system, just as if they were regular frequency ratios. If the $\mathbf{w}'$ coordinate system is used for the calculations of the actions, the transverse action $\tilde{I}_1'$ is found to vanish close to S^+, whereas both $\tilde{I}_1'$ and $\tilde{I}_2'$ remain non-zero in the vicinity of S^-. This demonstrates that locally the collapse of the T_2 onto S^+ and S^- looks the same when described in suitable coordinates. The nontrivial topology of the families T_2^{p} and T_2^{n} becomes visible only when the entire families, including both limiting FPOs, are studied.

The results in Fig. 2 were obtained for the energy $\tilde{E} = -1.5$, below the ionization threshold. If the energy is raised above the ionization threshold, to $\tilde{E} = -1.4$, as in the inset of Fig. 2, the FPO S^-, although still stable, is surrounded by a region of ionizing trajectories. Therefore, the T_2 cannot collapse onto S^- as they did below the threshold.

The 3-torus POs can be discussed in a similar manner. One of the three action variables ($\tilde{I}_3$) that characterize the T_3^{p} is displayed in Fig. 4. It depends mainly on $\frac{\tilde{\omega}_3}{\tilde{\omega}_2}$ and tends to zero at the lower boundary, which is the locus of the 2-torus POs T_2^{p}.

This allows us to identify I_3 as a transverse action variable that describes how the T_3 shrink onto the T_2 as the limit is approached. In the same limit, $\tilde{I}_1$ and $\tilde{I}_2$ tend toward the values obtained from the 2-torus POs and shown in Fig. 2.

3. Torus quantization

With the phase space topology and the action variables at hand we are now ready to calculate semiclassical eigenvalues of the crossed-fields hydrogen atom via EBK torus quantization.

The phase space volume filled with 3-torus POs from the T_3^{p} family is considerably larger than the volume filled with T_3^{n}, as can be seen by the number of respective POs for example in Fig. 1. Thus, the largest part of the EBK spectrum is also obtained from the quantization of the actions belonging to T_3^{p}.

The EBK quantization condition reads [12–14, 27]:

$$I_i = \oint_{\gamma_i} \mathbf{p} d\mathbf{q} = 2\pi\hbar \left(n_i + \frac{\alpha_i}{4} \right) \quad , \qquad i = 1, 2, 3 \tag{2}$$

with n_i being the semiclassical quantum number and α_i the Maslov indices. In our case, the action integral is given by the scaled action variables $\tilde{I}_i$, which need to be rescaled by a factor of $B^{-1/3}$ to obtain the true action $I = \tilde{I} B^{-1/3}$. Thus our quantization condition reads with $\hbar = 1$ in atomic units:

$$\tilde{I}_i \left(\frac{w_1}{w_2}, \frac{w_3}{w_2} \right) = 2\pi \left(n_i + \frac{\alpha_i}{4} \right) B^{1/3}. \tag{3}$$

We derive the Maslov indices α_i from two simple considerations. Namely, $\tilde{I}_2$ corresponds in the limit to the revolution on the two FPOs, which clearly has rotational character and requires $\alpha_2 = 0$. The other two modes are trans-

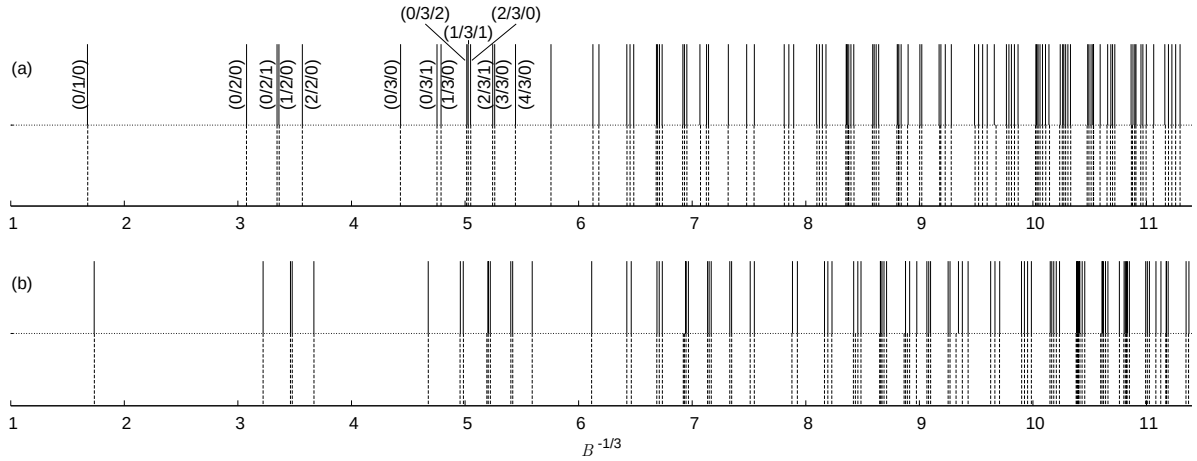

FIG. 3. (a) the EBK spectrum as obtained from the quantization of the T_3^{p} (solid) at $\tilde{F} = 0.5$ and $\tilde{E} = -1.4$ compared to the exact quantum-mechanical spectrum (dashed). The first three n_2-manifolds are labelled with (n_1, n_2, n_3). (b) the same at $\tilde{E} = -1.5$.

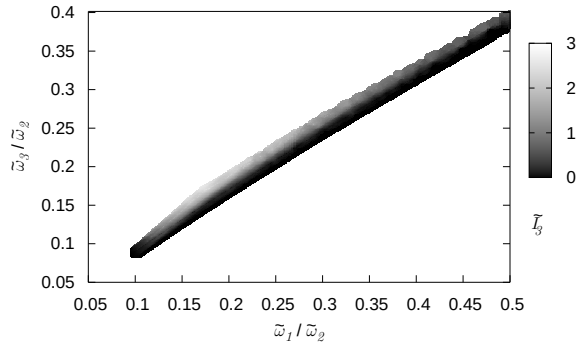

FIG. 4. Action variable $\tilde{I}_3$ for the T_3^{p} family at $\tilde{E} = -1.4$.

verse to this fundamental motion and thus expected to have vibrational character leading to $\alpha_1 = \alpha_3 = 2$. Comparisons of the EBK spectra with exact quantum spectra [28–31] at $\tilde{F} = 0.5$ and scaled energies $\tilde{E} = -1.4$ and $\tilde{E} = -1.5$ are given in Fig. 3. The agreement is excellent.

4. Conclusion

In summary, we have demonstrated how periodic orbits can be used to reconstruct a hierarchy of phase space structures in a strongly coupled multidimensional Hamiltonian system. The calculation of the associated action variables provides the key prerequisite for an Einstein-Brillouin-Keller torus quantization that the crossed-fields hydrogen atom has so far resisted. Since the method presented here relies solely on the periodic orbits as the backbone of the phase space structure, it will be available even at high energies where the phase space is partially chaotic.

We have carried out Poincaré's 1892 dictum to use periodic orbits as an entrée into the "the place [...] thought to be inaccessible". Indeed, it is remarkable how much the organization of these seemingly mundane objects reveals about the global phase space structure of multidimensional systems.

Acknowledgments

We thank T. Uzer for stimulating discussions. We also thank the DFG, DAAD and the Alexander von Humboldt Foundation for financial support.

References

[1] H. Poincaré, *Les méthodes nouvelles de la mécanique céleste*, volume 1, chapter III, page 82, Imprimerie Gauthier-Villars et fils, Paris, 1892, [authors' translation].

[2] V. Szebehely, *Theory of orbits*, Academic Press, 1967.

[3] F. Gabern and À. Jorba, Discrete Contin. Dynam. Systems Series B **1**, 143 (2001).

[4] R. Prosmiti and S. C. Farantos, J. Chem. Phys. **118**, 8275 (2003).

[5] F. J. Arranz, R. M. Benito, and F. Borondo, J. Chem. Phys. **123**, 044301 (2005).

[6] O. Hahn, J. M. G. Llorente, and H. S. Taylor, J. Chem. Phys. **94**, 2608 (1991).

[7] D. Robin, C. Steier, J. Laskar, and L. Nadolski, Phys. Rev. Lett. **85**, 558 (2000).

[8] M. C. Gutzwiller, *Chaos in Classical and Quantum Mechanics*, Springer, New York, 1990.

[9] G. Raithel, M. Fauth, and H. Walther, Phys. Rev. A **44**, 1898 (1991).

[10] D. M. Wang and J. B. Delos, Phys. Rev. A **63**, 043409 (2001).

[11] G. Kawahara and S. Kida, J. Fluid. Mech. **449**, 291 (2001).

[12] A. Einstein, Verh. Dtsch. Phys. Ges. **19**, 82 (1917).

[13] L. Brillouin, J. Phys. Radium **7**, 353 (1926).

[14] J. B. Keller, Ann. Phys. (NY) **4**, 180 (1958).

[15] G. Stania and H. Walther, Phys. Rev. Lett. **95**, 194101 (2005).

[16] E. Flöthmann and K. H. Welge, Phys. Rev. A **54**, 1884 (1996).

[17] C. Jaffé et al., Phys. Rev. Lett. **89**, 011101 (2002).

[18] M. M. Dignam and J. E. Sipe, Phys. Rev. B **45**, 6819 (1992).

[19] E. Lee, A. Puzder, M. Y. Chou, T. Uzer, and D. Farrelly, Phys. Rev. B **57**, 12281 (1998).

[20] V. I. Arnold, *Mathematical Methods of Classical Mechanics*, Springer, 1989.

[21] E. Tannenbaum and E. J. Heller, J. Phys. Chem. A **105**, 2803 (2001).

[22] C. C. Martens and G. S. Ezra, J. Chem. Phys **86**, 279 (1987).

[23] H. Kook and J. D. Meiss, Physica D **35**, 65 (1989).

[24] H. Friedrich, Scaling properties for atoms in external fields, in *Atoms and Molecules in Strong External Fields*, edited by P. Schmelcher and W. Schweizer, pages 153–167, Plenum Press, New York, 1998.

[25] E. Flöthmann, J. Main, and K. H. Welge, J. Phys. B **27**, 2821 (1994).

[26] S. Gekle, J. Main, T. Bartsch, and T. Uzer, Extracting multidimensional phase space topology from periodic orbits, submitted.

[27] M. Brack and R. K. Bhaduri, *Semiclassical physics*, Westview Press, 2003.

[28] J. Main and G. Wunner, J. Phys. B **27**, 2835 (1994).

[29] J. Rao, D. Delande, and K. T. Taylor, J. Phys. B **34**, L391 (2001).

[30] J. Main and G. Wunner, Phys. Rev. Lett. **69**, 586 (1992).

[31] P. A. Braun and E. A. Solovev, Sov. Phys. JETP **59**, 38 (1984).